Bubble acoustical scattering cross section under multi-frequency acoustic excitation*

Jie Shi(时洁)[1,2], De-sen Yang(杨德森)[1,2], Hao-yang Zhang(张昊阳)[1,2,†], Sheng-guo Shi(时胜国)[1,2], Song Li(李松)[1,2], and Bo Hu(胡博)[1,2]

[1] *Acoustic Science and Technology Laboratory, Harbin Engineering University, Harbin* 150001, *China*
[2] *College of Underwater Acoustic Engineering, Harbin Engineering University, Harbin* 150001, *China*

(Received 8 February 2017; revised manuscript received 13 March 2017; published online 17 May 2017)

The acoustical scattering cross section is usually employed to evaluate the scattering ability of the bubbles when they are excited by the incident acoustic waves. This parameter is strongly related to many important applications of performance prediction for search sonar or underwater telemetry, acoustical oceanography, acoustic cavitation, volcanology, and medical and industrial ultrasound. In the present paper, both the analytical and numerical analysis results of the acoustical scattering cross section of a single bubble under multi-frequency excitation are obtained. The nonlinear characteristics (e.g., harmonics, subharmonics, and ultraharmonics) of the scattering cross section curve under multi-frequency excitation are investigated compared with single-frequency excitation. The influence of several paramount parameters (e.g., bubble equilibrium radius, acoustic pressure amplitude, and acoustic frequencies) in the multi-frequency system on the predictions of scattering cross section is discussed. It is shown that the combination resonances become significant in the multi-frequency system when the acoustic power is big enough, and the acoustical scattering cross section is promoted significantly within a much broader range of bubble sizes and acoustic frequencies due to the generation of more resonances.

Keywords: acoustical scattering cross section, bubbles, multi-frequency excitaion, nonlinear characteristics

PACS: 43.25.Rq, 43.25.Ts, 43.25.Yw **DOI:** 10.1088/1674-1056/26/7/074301

1. Introduction

Gas bubbles play an important role in the generation, scattering, and absorption of sound in a liquid. The acoustical scattering cross section is usually employed to evaluate the scattering ability of the bubbles, and is defined as the square of the ratio between the amplitude of the radiated spherical wave by bubbles and the amplitude of the incident acoustic wave. Compared with the scattering behavior of incompressible objects, the acoustical scattering cross section of bubbles is quite significant due to the compressible nature of the gases inside the bubbles, and the scattering cross section of bubbles under acoustic excitation can be of the order of 1000 times of its own geometrical cross section.[1,2]

The acoustical scattering cross section of gas bubbles has been studied over several decades. Linear models of bubble scattering cross sections are used to measure oceanic bubble size distributions and predict their acoustic effects, with applications involving sonar performance,[3,4] and surf zone or subsurface acoustics.[5,6] A paper by Ainslie[1] has reviewed expressions and definitions in the literature for acoustical cross sections, resonance frequencies, and damping factors of a spherically pulsating gas bubble in an infinite liquid medium. The survey of bubble scattering models can be ordered into three threads, referred to as the "Wildt" thread, the "Devin" thread, and a third "nonlinear" thread. Zhang also proposed a generalized equation for the scattering cross section of spherical gas bubbles oscillating in liquids under acoustic excitation.[7] Shi *et al.* studied the oscillation properties influenced by stimulated sound scattering processes.[8] For the cases of bubble clouds, both the velocity and amplitude of the acoustic waves will be modulated due to the presence of bubbles. Similarly, the velocity and amplitude of the spherical waves generated by the oscillating bubbles will also be changed by the other bubbles.[9] For the linear case, Commander and Prosperetti[10] performed a systematic theoretical study. For a spherical bubble cloud, the acoustical scattering cross section could be theoretically calculated following the framework of d'Agostino and Brennen.[11]

The previous investigations detailed in the literature mainly focused on the case of single-frequency acoustic excitation. However, to promote acoustic effects in many application areas, the multi-frequency approach (i.e., waves with two or three, even more acoustic components) could be an effective method.[12] The multi-frequency approach has been employed to measure the bubble density in water,[13–15] find the bubble size distributions with void fraction in the ocean,[16,17] optimize the scattering from a micro bubble at a frequency different from the driving,[18] and advance the biomedical ultrasound imaging techniques.[19] Zhang *et al.* focused on the

*Project supported by the National Natural Science Foundation of China (Grant No. 11674074) and the Program for Changjiang Scholars and Innovative Research Team in University, China (Grant No. IRT1228).

†Corresponding author. E-mail: zhanghaoyang@hrbeu.edu.cn

© 2017 Chinese Physical Society and IOP Publishing Ltd

dual-frequency approach to obtain the influence of mass transfer on the oscillations of cavitation bubbles, and proposed a threshold of acoustic pressure amplitude dividing the bubble response into two regions.[20] Furthermore, Zhang *et al.* studied the acoustical scattering cross section, and the combination and simultaneous resonances of gas bubbles under dual-frequency acoustic excitation in detail.[21–23]

However, the problems of acoustical cross section of a bubble under multi-frequency excitation are still poorly investigated in the literature. The motivation of this paper is to achieve a much broader range of acoustical scattering cross section by the multi-frequency approach. Different from the work of Zhang *et al.*,[21–24] our work improves the dual-frequency approach to the multi-frequency approach. The main aim of the paper is to obtain directly the analytical solution of the acoustical scattering cross section under multi-frequency excitation, and make a comprehensive analysis of the influence of several paramount parameters (e.g., bubble equilibrium radius, acoustic pressure amplitude, and acoustic frequencies) in the multi-frequency system.

The remainder of the article is organized as follows. In Section 2, the equations relating with the acoustical scattering cross section of gas bubbles under multi-frequency acoustic excitation are obtained by both analytical and numerical solutions. In Section 3, the nonlinear nature of the acoustical scattering cross section of gas bubbles under multi-frequency acoustic waves is revealed. The influences of several paramount parameters (e.g., bubble equilibrium radius, acoustic pressure amplitude, and acoustic frequencies) on the scattering cross section are shown. The conclusions are summarized in Section 4.

2. Basic equations

The dynamics of spherical gas bubbles in Newtonian, compressible, and viscous liquids are considered, and the equation of bubble motion can be written as the Keller–Miksis equation[25,26]

$$\left(1-\frac{\dot{R}}{c}\right)R\ddot{R}+\frac{3}{2}\left(1-\frac{\dot{R}}{3c}\right)\dot{R}^2 = \left(1+\frac{\dot{R}}{c}\right)\frac{p_{\rm ext}(R,t)-p_{\rm s}(t)}{\rho} + \frac{R}{\rho c}\frac{{\rm d}[p_{\rm ext}(R,t)-p_{\rm s}(t)]}{{\rm d}t}, \quad (1)$$

$$p_{\rm ext}(R,t)=\left(P_0+\frac{2\sigma}{R_{\rm n}}\right)\left(\frac{R_{\rm n}}{R}\right)^{3\kappa}-\frac{2\sigma}{R}-\frac{4\eta}{R}\dot{R}, \quad (2)$$

$$P_0=P_{\rm stat}-P_{\rm V}, \quad (3)$$

where R is the instantaneous bubble radius; the overdot denotes the time derivative; t is the time; ρ, c, η, and σ are the density, the speed of sound in the liquid, the viscosity of the liquid, and the coefficient of surface tension, respectively; P_0 is the ambient pressure; $P_{\rm stat}$ is the static pressure of the environment; $P_{\rm V}$ is the vapor pressure inside the bubble; $R_{\rm n}$ is the equilibrium bubble radius; κ is the polytropic exponent; and $p_{\rm s}(t)$ is the pressure outside the bubble at the bubble wall.

For multi-frequency excitation, $p_{\rm s}(t)$ in Eq. (1) can be expressed as

$$p_{\rm s}(t)=P_0\left(1+\sum_{k=1}^{K}\varepsilon_k\cos(\omega_k t)\right). \quad (4)$$

Assume the amplitudes of the acoustic wave as $P_{{\rm A}k}$ ($k=1,2,\ldots,K$), respectively, $\varepsilon_k=P_{{\rm A}k}/P_0$ are the non-dimensional amplitudes of the external acoustic excitation using the ambient pressure. The ratio of the pressure amplitudes of the multi-frequency acoustic waves is defined as $\psi_k=P_{{\rm A}k}/P_{\rm A1}$, which reflects the power allocation between each high-frequency component and the lowest frequency component. We set $\psi_k=1$. $\omega_k=2\pi f_k$ are the angular frequencies of the external acoustic excitation.

The radiation pressure at radial coordinate r from the origin of the bubble center can be given as[27]

$$P_{\rm rad}(r,t)=\frac{\rho R}{r}\left(2\dot{R}^2+R\ddot{R}\right), \quad (5)$$

where $P_{\rm rad}$ is the radiation pressure, and r is the radial coordinate with the origin at the bubble center. The solution of the bubble motion can be obtained by solving Eqs. (1)–(4), i.e., the dynamic oscillations of R, $\dot{R}$, and $\ddot{R}$. Substituting the above solutions into Eq. (5), the radiation pressure generated by the bubble oscillations can be obtained. The amplitude of the radiation pressure can be written as

$$|P_{\rm rad}|=\left|\frac{B}{r}\right|. \quad (6)$$

Here, B/r is the amplitude of the divergent spherical scattered wave generated by the bubble oscillations. Following the definition proposed by Wildt,[2] the acoustical scattering cross section ($\sigma_{\rm s}$) of an oscillating gas bubble in the liquid, which reflects the square of the ratio between scattered waves and incident waves, can be defined as

$$\sigma_{\rm s}=4\pi|B/A|^2, \quad (7)$$

where A is the amplitude of the incident wave. Hence, $\sigma_{\rm s}$ reflects the scattering ability of gas bubbles when they are excited by acoustic waves.

2.1. Analytical analysis

The analytical solution for the acoustical scattering cross section under multi-frequency acoustic excitation is obtained in this section. The solution of the Keller–Miksis equation under multi-frequency acoustic field can be expressed as

$$\frac{R}{R_{\rm n}}=1+\varepsilon x_1+\varepsilon^2 x_2. \quad (8)$$

Thermal damping is ignored. Substituting Eq. (8) to Eq. (1), we obtain the following equation by considering the terms up to the first order of ε:

$$
\begin{aligned}
&R_{\mathrm{n}}^2\left[\varepsilon\ddot{x}_1+\varepsilon^2\left(\ddot{x}_2+x_1\ddot{x}_1-\frac{R_{\mathrm{n}}}{c}\dot{x}_1\ddot{x}_1\right)\right]+\frac{3}{2}R_{\mathrm{n}}^2\varepsilon^2\dot{x}_1^2\\
&-\frac{\varepsilon}{\rho}\left[-3\kappa\left(P_0+\frac{2\sigma}{R_{\mathrm{n}}}\right)x_1+\frac{2\sigma}{R_{\mathrm{n}}}x_1\right.\\
&\left.-P_0\sum_{k=1}^{K}\varepsilon_k\cos(\omega_k t)-4\mu\dot{x}_1\right]\\
&-\frac{\varepsilon R_{\mathrm{n}}}{\rho c}\left[-3\kappa\left(P_0+\frac{2\sigma}{R_{\mathrm{n}}}\right)\dot{x}_1+\frac{2\sigma}{R_{\mathrm{n}}}\dot{x}_1\right.\\
&\left.+P_0\sum_{k=1}^{K}\varepsilon_k\omega_k\sin(\omega_k t)-4\mu\ddot{x}_1\right]\\
&-\frac{\varepsilon^2}{\rho}\left\{\left[-3\kappa\left(P_0+\frac{2\sigma}{R_{\mathrm{n}}}\right)+\frac{2\sigma}{R_{\mathrm{n}}}\right]x_2\right.\\
&+\left[\frac{3\kappa(3\kappa+1)}{2}\left(P_0+\frac{2\sigma}{R_{\mathrm{n}}}\right)-\frac{2\sigma}{R_{\mathrm{n}}}\right]x_1^2-4\mu\left(\dot{x}_2-x_1\dot{x}_1\right)\Big\}\\
&-\frac{\varepsilon^2 R_{\mathrm{n}}}{\rho c}\left\{-3\kappa\left(P_0+\frac{2\sigma}{R_{\mathrm{n}}}\right)\dot{x}_2+3\kappa(3\kappa+1)\left(P_0+\frac{2\sigma}{R_{\mathrm{n}}}\right)x_1\dot{x}_1\right.\\
&+\frac{2\sigma}{R_{\mathrm{n}}}\left(\dot{x}_2-2x_1\dot{x}_1\right)-4\mu\left(-\dot{x}_1^2+\ddot{x}_2-x_1\ddot{x}_1\right)\\
&+x_1\left[-3\kappa\left(P_0+\frac{2\sigma}{R_{\mathrm{n}}}\right)\dot{x}_1+\frac{2\sigma}{R_{\mathrm{n}}}\dot{x}_1\right.\\
&\left.+P_0\sum_{k=1}^{K}\varepsilon_k\omega_k\sin(\omega_k t)-4\mu\ddot{x}_1\right]\\
&+\dot{x}_1\left[-3\kappa x_1\left(P_0+\frac{2\sigma}{R_{\mathrm{n}}}\right)+\frac{2\sigma}{R_{\mathrm{n}}}x_1\right.\\
&\left.\left.-P_0\sum_{k=1}^{K}\varepsilon_k\cos(\omega_k t)-4\mu\dot{x}_1\right]\right\}=0. \qquad (9)
\end{aligned}
$$

The sum of all terms with order ε in the above equation should be equal to zero respectively. The result can be expressed as

$$
\begin{aligned}
&\ddot{x}_1+2\beta_{\mathrm{tot}}\dot{x}_1+\omega_{\mathrm{n}}^2x_1\\
&=-\frac{P_0}{M\rho R_{\mathrm{n}}^2}\sum_{k=1}^{K}\varepsilon_k\left(\cos(\omega_k t)-\frac{\omega_k R_{\mathrm{n}}}{c}\sin(\omega_k t)\right), \qquad (10)
\end{aligned}
$$

where

$$M=1+\frac{R_{\mathrm{n}}}{c}\frac{4\eta}{\rho R_{\mathrm{n}}^2}, \qquad (11)$$

$$\beta_{\mathrm{tot}}=\beta_{\mathrm{vis}}+\beta_{\mathrm{ac}}=\frac{2\mu}{M\rho R_{\mathrm{n}}^2}+\frac{R_{\mathrm{n}}}{2c}\omega_{\mathrm{n}}^2, \qquad (12)$$

$$\omega_{\mathrm{n}}^2=\frac{1}{M\rho R_{\mathrm{n}}^2}\left[3\kappa\left(P_0+\frac{2\sigma}{R_{\mathrm{n}}}\right)-\frac{2\sigma}{R_{\mathrm{n}}}\right]. \qquad (13)$$

The solution of Eq. (10) can be written as

$$x_1=\sum_{k=1}^{K}A_k\cos(\omega_k t+\delta_k), \qquad (14)$$

where

$$A_k=-\frac{P_0\psi_k}{M\rho R_{\mathrm{n}}^2}\sqrt{\frac{1+(\omega_k R_{\mathrm{n}}/c)^2}{(\omega_{\mathrm{n}}^2-\omega_k^2)^2+4\beta_{\mathrm{tot}}^2\omega_k^2}}, \qquad (15)$$

$$\delta_k=\tan^{-1}\left\{\frac{\frac{\omega_k R_{\mathrm{n}}}{c}(\omega_{\mathrm{n}}^2-\omega_k^2)-2\beta_{\mathrm{tot}}\omega_k}{(\omega_{\mathrm{n}}^2-\omega_k^2)+2\beta_{\mathrm{tot}}\omega_k^2\frac{R_{\mathrm{n}}}{c}}\right\}. \qquad (16)$$

Here, ω_{n} is the natural frequency of the gas bubbles oscillating in the liquids; β_{tot}, β_{vis}, and β_{ac} are the total, viscous, and acoustic damping constants, respectively. Therefore, the acoustical scattering cross section under multi-frequency excitation is

$$\sigma_{\mathrm{s}}=4\pi|B/A|^2=4\pi\left(\frac{\rho R_{\mathrm{n}}^3}{P_0}\right)^2\frac{\sum_{k=1}^{K}A_k^2\omega_k^4}{\sum_{k=1}^{K}\psi_k^2}. \qquad (17)$$

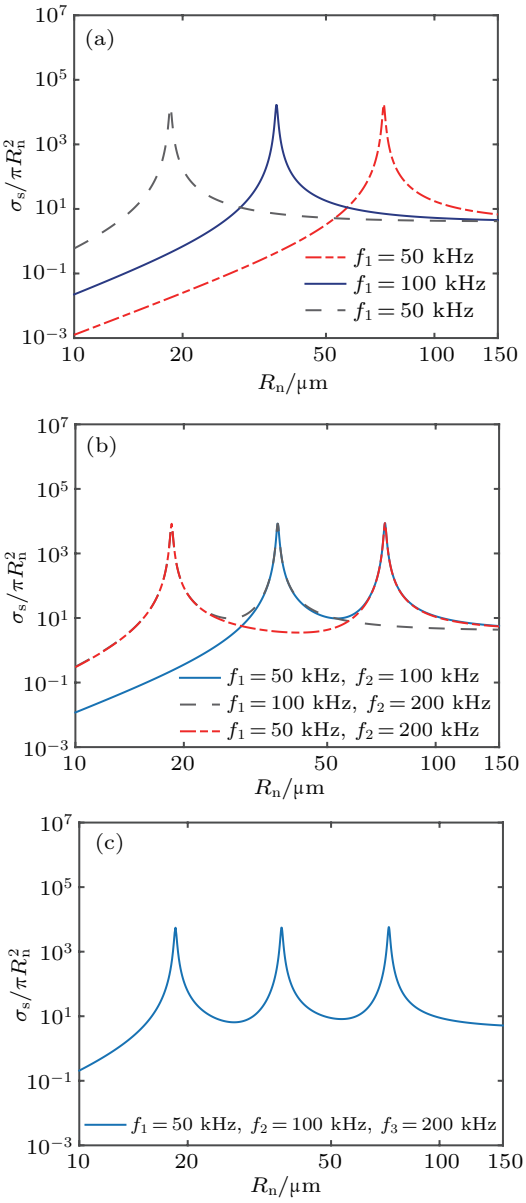


Fig. 1. (color online) Prediction of acoustical scattering cross section against equilibrium bubble radius under single-frequency, dual-frequency and tri-frequency acoustic excitations by analytical solution: (a) acoustic excitation versus different single-frequency, (b) acoustic excitation versus different dual-frequency, and (c) tri-frequency acoustic excitation. $P_{\mathrm{tot}}=0.1P_0$, $\psi_k=1$ $(k=1,2,3)$.

The typical parameters for a bubble in water, as used in the calculations with the Keller–Miksis model, are $R|_{t=0} = R_n$, $dR/dt|_{t=0} = 0$, $\rho = 998$ kg/m^3, $\sigma = 0.0725$ N/m, $\eta = 0.001$ Pa·s, $P_{stat} = 103.6$ kPa, $P_V = 2.33$ kPa, $P_0 = P_{stat} - P_V = 101.3$ kPa, $c = 1500$ m/s, and $\kappa = 4/3$. For simplicity, the acoustical scattering cross sections of individual bubbles are normalized by their respective geometrical cross sections, i.e., $\sigma_s/(\pi R_n^2)$.

For comparison, the total input power should be a constant during simulations of different cases, so we can obtain the acoustic pressure amplitude during different cases

$$P_{tot} = \sqrt{\sum_{k=1}^{K} P_{Ak}^2} = P_0 \sqrt{\sum_{k=1}^{K} \varepsilon_k^2}. \tag{18}$$

Figure 1 shows the acoustical scattering cross section (i.e., curves of $\sigma_s/(\pi R_n^2)$ against equilibrium bubble radius) predicted by Eq. (17) under single-frequency excitation, dual-frequency excitation (different combinations of frequencies), and tri-frequency excitation ($f_1 = 50$ kHz, $f_2 = 100$ kHz, and $f_3 = 200$ kHz), respectively. However, the analytical solution can give the main resonances clearly, but cannot predict complex nonlinear phenomena when P_{tot} is big enough.

2.2. Numerical analysis

Next, the numerical solution is employed to study the acoustical scattering cross section generated by bubble oscillations. The Keller–Miksis equation can be reformulated as a set of autonomous differential equations of first order

$$\dot{R} = U, \tag{19}$$

$$\begin{aligned}\dot{U} = {} & \left[-\frac{U^2}{2}\left(3 - \frac{U}{c}\right) + \left(1 + (1-3\kappa)\frac{U}{c}\right) \right. \\ & \times \left(\frac{P_0}{\rho} + \frac{2\sigma}{\rho R_n}\right)\left(\frac{R_n}{R}\right)^{3\kappa} - \frac{4\mu}{\rho}\frac{U}{R} - \frac{2\sigma}{\rho R} \\ & - \left(1 + \frac{U}{c}\right)\frac{P_0\left(1 + \sum_{k=1}^{K}\varepsilon_k \cos(2\pi f_k t - \theta_k)\right)}{\rho} \\ & \left. + \frac{R}{\rho c} P_0 \sum_{k=1}^{K} \varepsilon_k 2\pi f_k \sin(2\pi f_k t - \theta_k) \right] \left[\left(1 - \frac{U}{c}\right) R + \frac{4\eta}{\rho c} \right]^{-1},\end{aligned} \tag{20}$$

$$\dot{\theta}_k = f_k, \tag{21}$$

where the variable is introduced for eliminating variable t. This equation can be directly solved using an explicit Runge–Kutta formula. For this bubble oscillation model, the main parameters of interest are the equilibrium bubble radius R_n, acoustic frequency f_k, and acoustic pressure amplitude P_{Ak}. The other parameters are connected with the properties of the liquid outside the bubble and the gas and vapor of the liquid inside the bubble. In the present paper, the origin of the coordinate is placed at the center of the bubble. In numerical simulations, the acoustical scattering cross section is evaluated at the point with distance $r = 10^{-3}$ m from the origin.

3. Result and discussion

In this section, demonstrating examples of radiation pressure and acoustical scattering cross section generated by an oscillating bubble under multi-frequency acoustic excitation within a wide range of parameters are shown. The nonlinear characteristics and influential parameters of the acoustical cross section are discussed in detail.

3.1. The instantaneous bubble radius and corresponding radiation pressure

Figure 2 demonstrates the variations of non-dimensional instantaneous bubble radius $(R - R_n)/R_n$ and radiation pressure P_{rad} versus time for 10 μm, 20 μm, 50 μm, and 100 μm bubbles oscillating under multi-frequency excitation respectively. For a certain $P_{tot} = 0.01P_0$, both the bubble oscillations and radiation pressure curves under single-, dual-, and tri-frequency excitations show obvious periodical oscillations. However, the bubble oscillations and the radiation pressure curves under dual-frequency and tri-frequency excitations exhibit much more complicated patterns owing to the involvement of extra frequency components. Additionally, the addition of the extra acoustic waves leads to great increases of the amplitude of the bubble oscillations and the radiation pressure when the equilibrium bubble radius R_n is not too big.

3.2. The characteristic of the scattering cross section under multi-frequency excitation

3.2.1. Influences of the pressure amplitude and the equilibrium bubble radius

Figure 3 shows the acoustical scattering cross section under single-frequency, dual-frequency, and tri-frequency acoustic excitations versus both equilibrium bubble radius R_n and acoustic pressure amplitude P_{tot} by numerical solution. A parameter plane, where only two parameters are varied, is best suited for viewing the details of the acoustical scattering cross section. This parameter space diagram (R_n, P_{tot}) is color coded, in which the driving pressure amplitude P_{tot} has been increased from $0.01P_0$ to $0.4P_0$, and the bubble radius R_n has been increased from 1 μm to 150 μm. The scale of acoustical scattering cross section $10\log(\sigma_s/(\pi R_n^2))$ is limited from −40 dB to 40 dB for different cases.

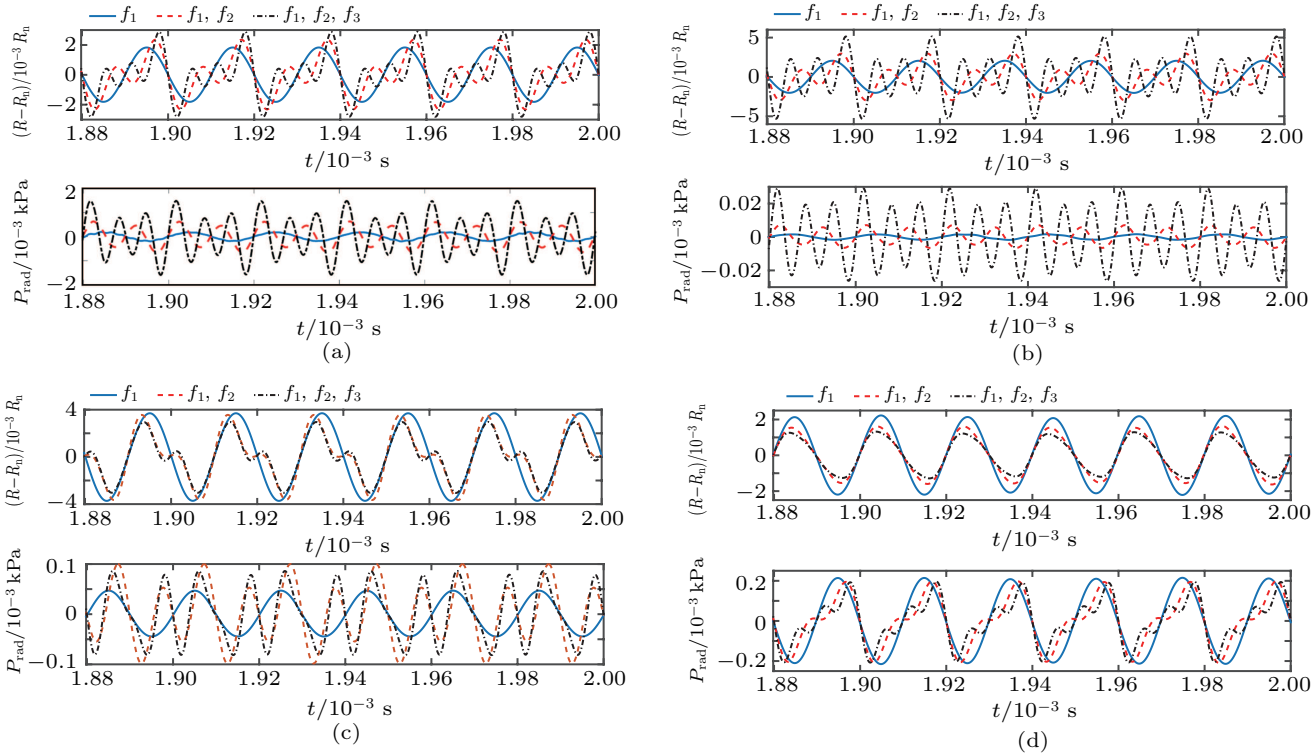


Fig. 2. (color online) The instantaneous bubble radius under the single-frequency acoustic excitation (solid line), dual-frequency acoustic excitation (dashed line), tri-frequency acoustic excitation (dash-dotted line) and the corresponding radiation pressure versus time for (a) 10 μm, (b) 20 μm, (c) 50 μm, and (d) 100 μm bubbles. $f_1 = 50$ kHz, $f_2 = 100$ kHz, $f_3 = f_1 + f_2 = 150$ kHz. $P_{tot} = 0.01P_0$, $\psi_k = 1$.

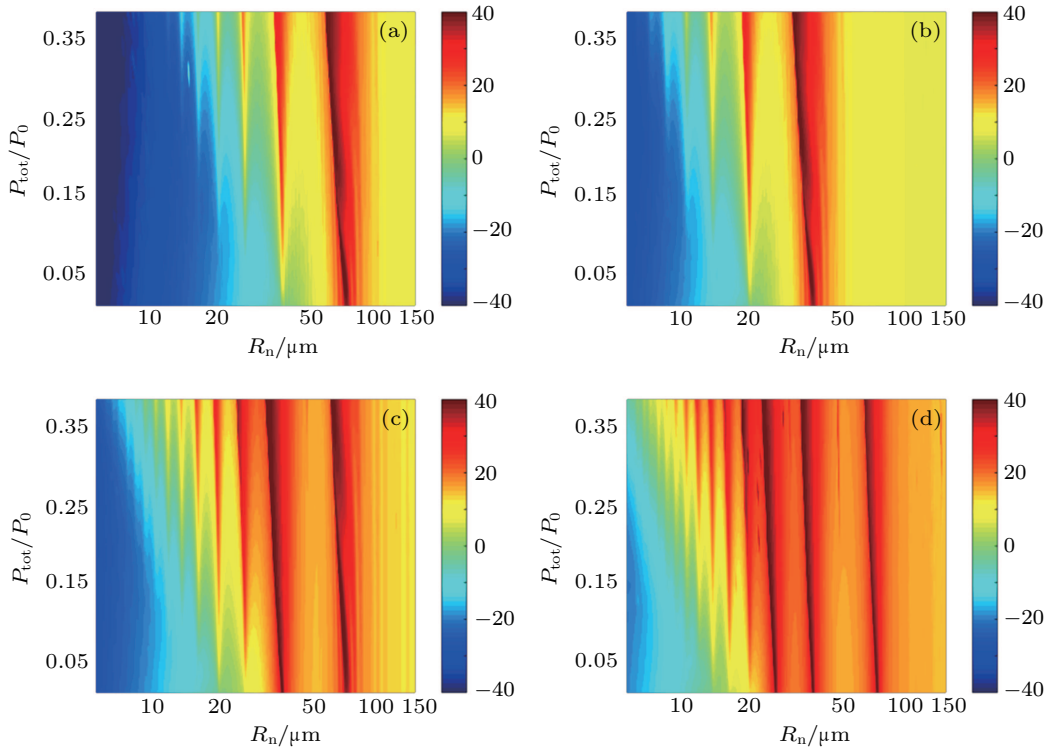


Fig. 3. (color online) Parameter space diagram spanned by R_n and P_{tot} giving the acoustical scattering cross section under single-frequency, dual-frequency, and tri-frequency acoustic excitations: (a) $f_1 = 50$ kHz; (b) $f_1 = 100$ kHz; (c) $f_1 = 50$ kHz, $f_2 = 100$ kHz; (d) $f_1 = 100$ kHz, $f_2 = 100$ kHz, $f_3 = 150$ kHz. The logarithmic bubble radius R_n scale stretches the acoustical scattering cross section for better viewing.

It is shown that the harmonics and subharmonics increase when driving the bubbles stronger in the case of single-frequency acoustic excitation. With the increase of P_{tot}, both the harmonic and subharmonic resonances grow significantly, and the peaks of these resonances bend toward smaller bubble radius. This bending phenomenon is a nonlinear feature determined by the Keller–Miksis equation.[24,25] In the case of multi-frequency acoustic excitation, the combination reso-

nances increase with the increase of the acoustic pressure amplitude and the number of the excitation frequency. It means that the acoustical scattering cross section is promoted significantly within a much broader range of bubble sizes and acoustic frequencies due to the generation of more resonances.

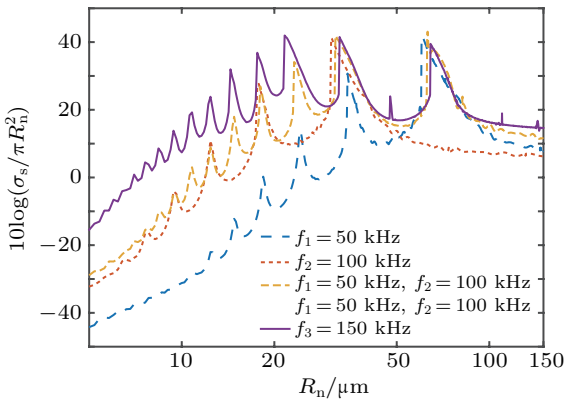


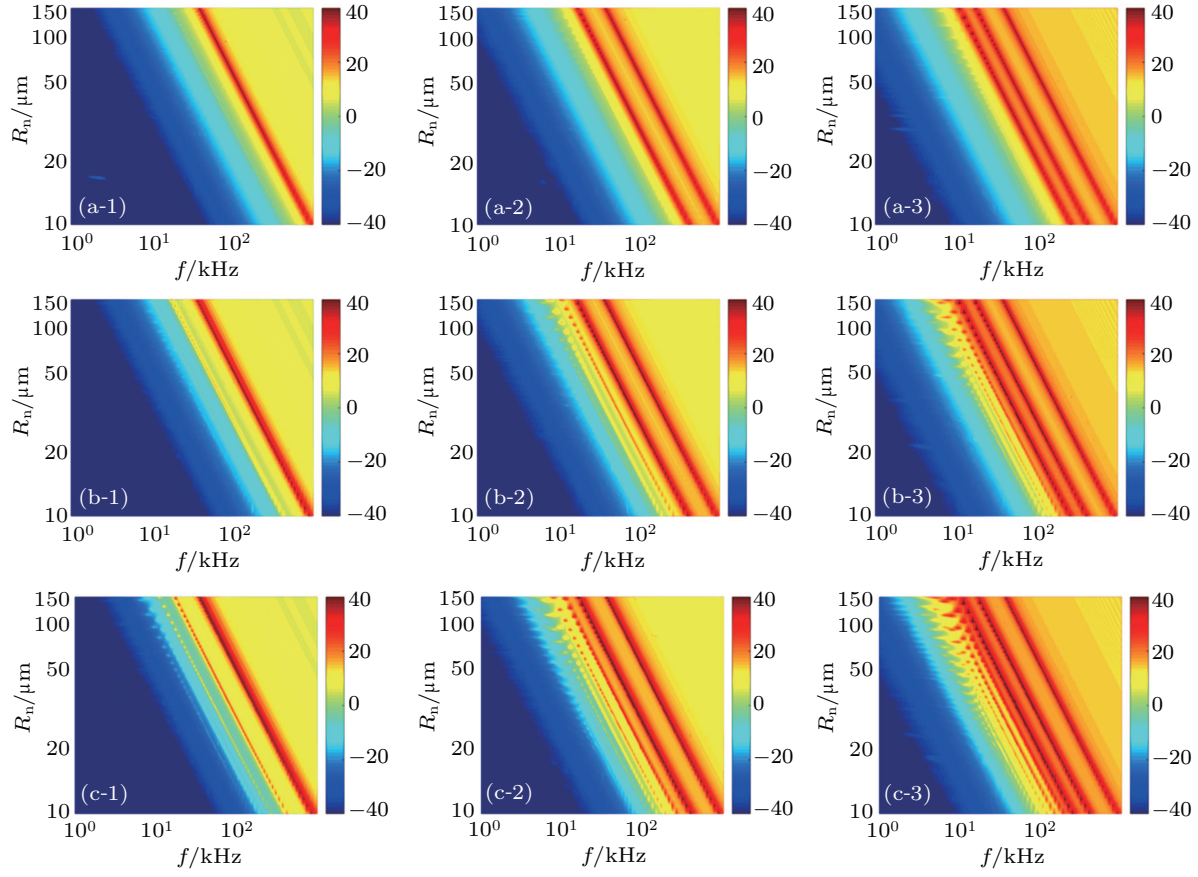
Fig. 4. (color online) The acoustical scattering cross section under single-frequency (dashed line $f_1 = 50$ kHz and dotted line $f_1 = 100$ kHz), dual-frequency (dash-dotted line $f_1 = 50$ kHz, $f_2 = 100$ kHz), and tri-frequency (solid line $f_1 = 100$ kHz, $f_2 = 100$ kHz, $f_3 = 150$ kHz) acoustic excitations versus equilibrium bubble radius by numerical solution. $P_{tot} = 0.3P_0$. The logarithmic bubble radius R_n scale stretches the acoustical scattering cross section cruves for better viewing.

Figure 4 shows a slice of Fig. 3 in the case of $P_{tot} = 0.3P_0$. Comparing the scattering cross section curves under single-frequency and multi-frequency excitations with the acoustic pressure amplitude $P_{tot} = 0.3P_0$, the amplitudes of the main resonances are not changed, but the harmonics, subharmonics, and the combination resonances increase with the increase of the number of the excitation frequency.

3.2.2. Influence of the frequency and the equilibrium bubble radius

Figure 5 shows the predicted scattering cross sections under single-frequency (first column), dual-frequency (second column), and tri-frequency (third column) excitations versus both excitation frequency f and equilibrium bubble radius R_n. In this parameter space diagram (f, R_n) (first column), the driving frequency f has been increased from 0 to 300 kHz, and the bubble radius R_n has been increased from 1 μm to 150 μm. In the cases of dual-frequency and tri-frequency excitions, the driving frequency f_1 has been increased from 0 to 300 kHz, and $f_2 = 0.5f_1$, $f_3 = 1.5f_1$.

In the case of single-frequency excitation, for a certain acoustic pressure amplitude P_{tot}, the scattering cross section reaches maximum when the bubble radius is equal to the resonant bubble radius corresponding to the driving frequency, i.e., at the main resonance. The scattering cross section curves show nonlinear features, such as harmonic, subharmonic, and ultraharmonic resonances. Compared to the single-frequency approach, the multi-frequency approach can generate much more resonance regions involving all the main, harmonic, and subharmonic resonances corresponding to the multiple component frequencies and a lot of combination resonances.



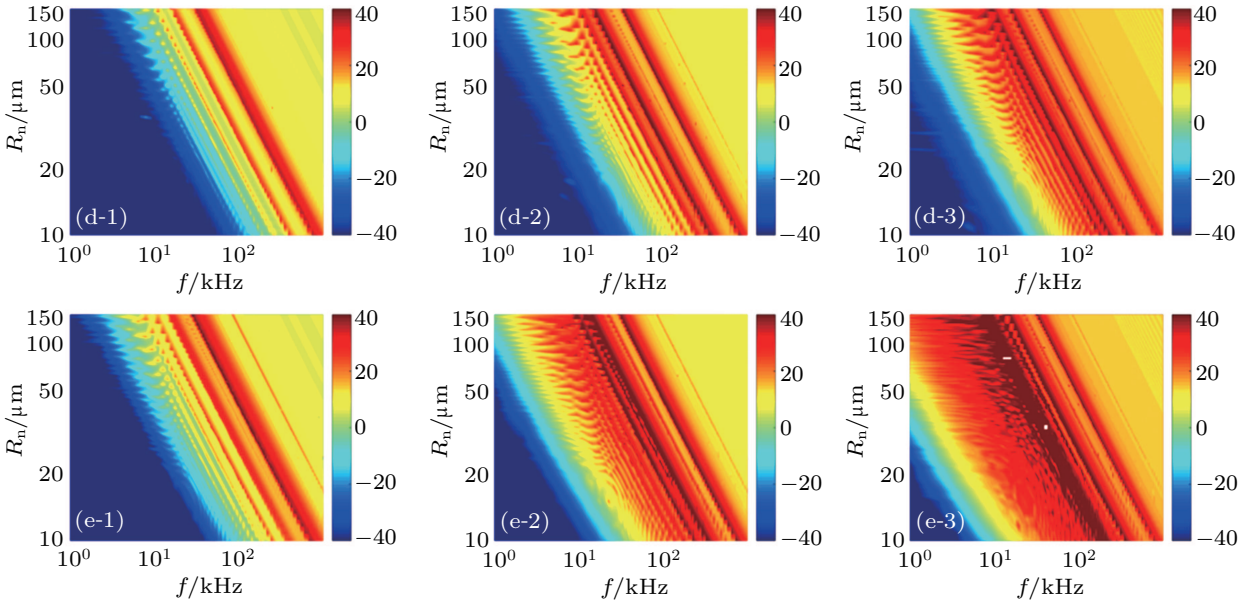
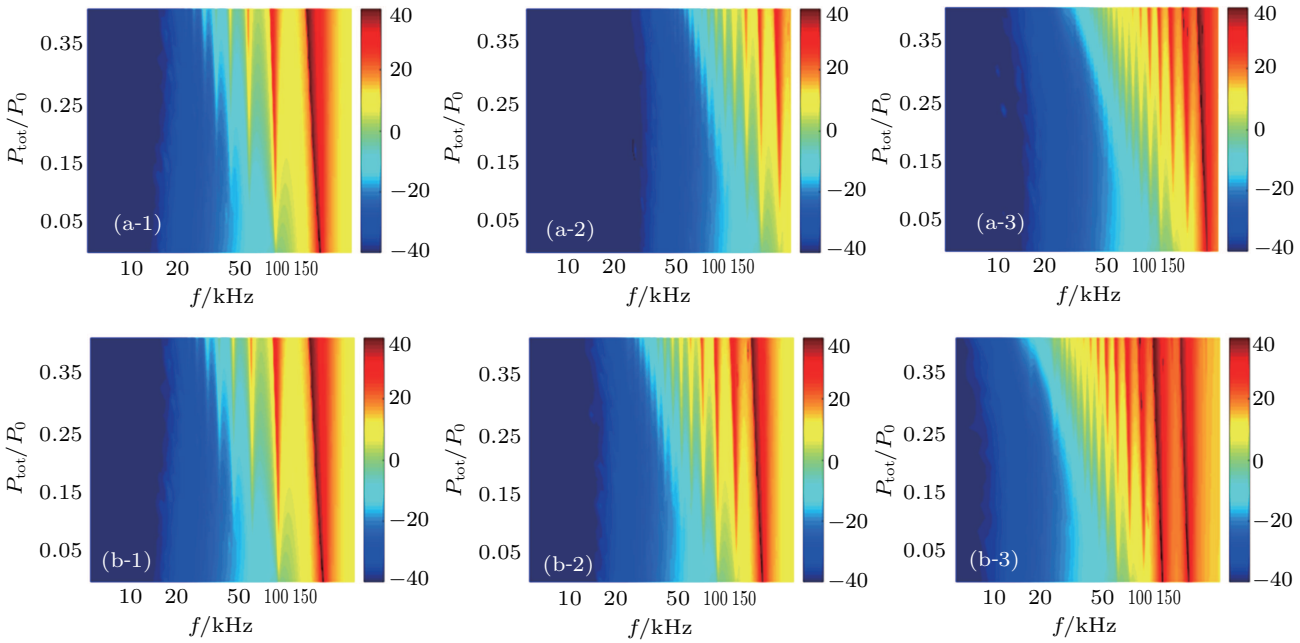


Fig. 5. (color online) The acoustical scattering cross section under single-frequency (first column), dual-frequency (second column), and tri-frequency (third column) acoustic excitations versus both excitation frequency f and equilibrium bubble radius R_n by numerical solution. (a) $P_{tot} = 0.01P_0$, (b) $P_{tot} = 0.1P_0$, (c) $P_{tot} = 0.2P_0$, (d) $P_{tot} = 0.4P_0$, (e) $P_{tot} = 0.6P_0$. The logarithmic bubble radius R_n scale and frequency f scale stretch the acoustical scattering cross section for better viewing.

3.2.3. Influence of the frequency and the pressure amplitude

Figure 6 shows the predicted scattering cross sections under single-frequency (first column), dual-frequency (second column) and tri-frequency (third column) excitations versus both excitation frequency f and acoustic pressure amplitude P_{tot}. In this parameter space diagram (f, P_{tot}) (first column), the driving frequency f has been increased from 0 to 300 kHz, and the acoustic pressure amplitude P_{tot} has been increased from $0.01P_0$ to $0.4P_0$. In the cases of dual-frequency and tri-frequency excitions, the driving frequency f_1 has been increased from 0 to 300 kHz, and $f_2 = 0.5f_1$, $f_3 = 1.5f_1$.

Compared to the single-frequency approach, for a certain bubble radius R_n, harmonic, subharmonic, and combination resonances become more and more complex with the increase of P_{tot} under the multi-frequency excitation.



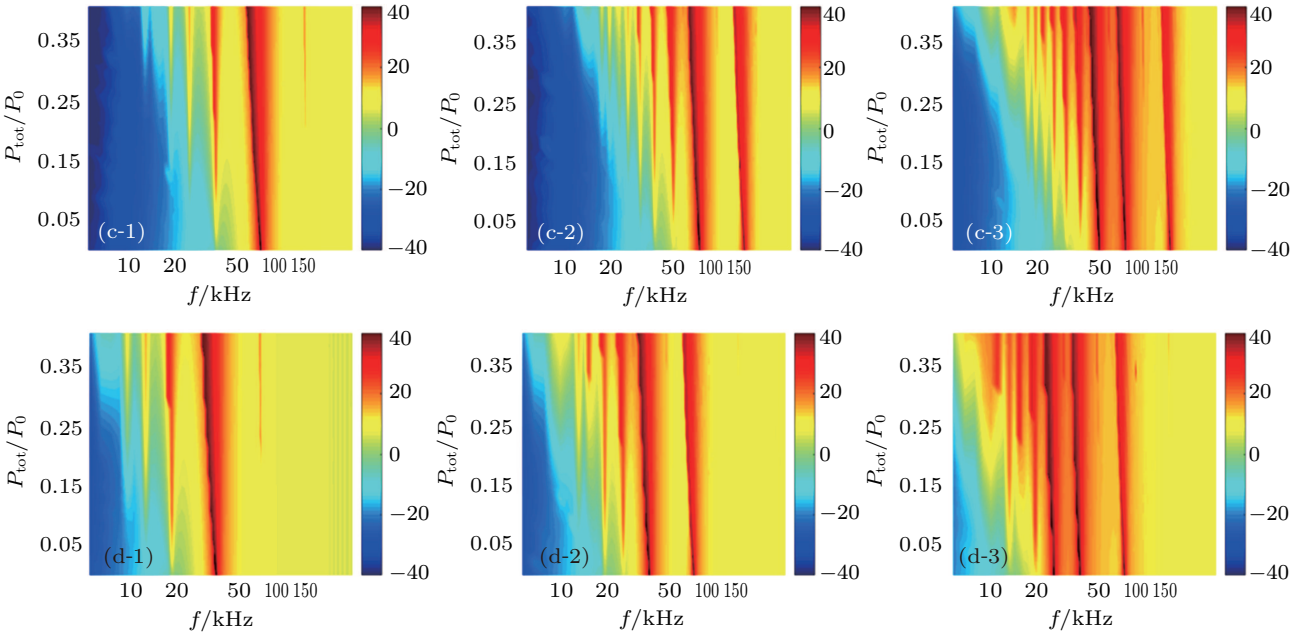


Fig. 6. (color online) The acoustical scattering cross section under single-frequency, dual-frequency, and tri-frequency acoustic excitations versus both excitation frequency f and P_{tot} by numerical solution. (a) $R_n = 10$ μm, (b) $R_n = 20$ μm, (c) $R_n = 50$ μm, (d) $R_n = 100$ μm. The logarithmic frequency f scale stretches the acoustical scattering cross section for better viewing.

4. Conclusion and perspectives

Both the analytical and numerical solutions of the acoustical scattering cross section of a bubble under multi-frequency excitation are obtained. The prediction of the scattering cross section by the analytical method can give the main resonances clearly, but cannot predict complex nonlinear phenomena when P_{tot} is big enough because many nonlinear features will present.

The nonlinear characteristics of the scattering cross section under the multi-frequency approach are investigated numerically by using parameter space diagrams (R_n, P_{tot}), (f, R_n), and (f, P_{tot}) in detail. Generally, the scattering cross section curves show typical nonlinear features such as harmonics, subharmonics, and ultraharmonics. Furthermore, the multi-frequency approach displays more resonances termed as combination resonances. Compared to the single-frequency approach, the multi-frequency approach could promote the acoustical scattering cross section significantly within a much broader range of bubble sizes due to the generation of more resonances.

The influence of several paramount parameters in the multi-frequency system on the scattering cross section has been discussed. Due to the vast parameter space, the properties of the scattering cross section are still not fully explored. Meanwhile, a large parameter zone is involved, leading to great difficulties for the design. So optimization of the multi-frequency approach is still needed and worth studying.

References

[1] Ainslie M A and Leighton T G 2011 *J. Acoust. Soc. Am.* **130** 3184

[2] Ainslie M A and Leighton T G 2009 *J. Acoust. Soc. Am.* **126** 2163

[3] Keiffer R S, Novarini J C and Norton G V 1997 *J. Acoust. Soc. Am.* **97** 227

[4] Trevorrow M V 2003 *J. Acoust. Soc. Am.* **114** 2672

[5] Vossen R V and Ainslie M A 2011 *J. Acoust. Soc. Am.* **130** 3413

[6] Vagle S and Farmer D M 1992 *J. Atmos. Oceanic Technol.* **9** 630

[7] Zhang Y N 2013 *J. Fluids Eng.* **135** 091301

[8] Shi J, Yang D S, Shi S G, Hu B, Zhang H Y and Hu S Y 2016 *Chin. Phys. B* **25** 024304

[9] Wijngaarden LV 1972 *Ann. Rev. Fluid Mech.* **4** 369

[10] Commander K W and Prosperetti A 1989 *J. Acoust. Soc. Am.* **85** 732

[11] d'Agostino L and Brennen C E 1988 *J. Acoust. Soc. Am.* **84** 2126

[12] Ma Q Y, Qiu Y Y, Huang B, Zhang D and Gong X F. 2010 *Chin. Phys. B* **19** 094301

[13] Newhouse V L and Shankar P M 1984 *J. Acoust. Soc. Am.* **75** 1473

[14] Phelps A D and Leighton T G 1994 *Investigations into the use of two frequency excitation to accurately determine bubble sizes, in: Bubble Dynamics and Interface Phenomena* (Springer, Netherlands) pp. 475–484

[15] Phelps A D, Ramble D G and Leighton T G 1997 *J. Acoust. Soc. Am.* **101** 1981

[16] Sutin A M, Yoon S W, Kim E J and Didenkulov I N 1998 *J. Acoust. Soc. Am.* **103** 2377

[17] Vagle S and Farmer D M 1998 *IEEE J. Oceanic Eng.* **23** 211

[18] Wyczalkowski M and Szeri A J 1998 *J. Acoust. Soc. Am.* **113** 3073

[19] Zheng H, Mukdadi O, Kim H, Hertzberg J R and Shandas R 2005 *Ultrasound Med. Biol.* **31** 99

[20] Zhang Y N 2012 *Int. Commun. Heat. Mass. Transf.* **39** 1496

[21] Zhang Y N, Du X, Xian H and Wu Y 2015 *Ultrason. Sonochem.* **23** 16

[22] Zhang Y N and Li S C 2015 *Ultrason. Sonochem.* **26** 437

[23] Zhang Y N and Li S C 2017 *Ultrason. Sonochem.* **35** 431

[24] Keller J B and Miksis M 1980 *J. Acoust. Soc. Am.* **68** 628

[25] Lauterborn W and Kurz T 2010 *Rep. Prog. Phys.* **73** 106501

[26] Zhang Y N 2012 *Analysis of Radial Oscillations of Gas Bubbles in Newtonian or Viscoelastic Mediums under Acoustic Excitation* (Ph. D. Thesis, University of Warwick)

[27] Naugolnykh K A and Ostrovsky L A 1998 *Nonlinear Wave Processes in Acoustics* (New York: Cambridge University Press) pp. 16–20, 261–265